The Canadian Mineralogist
Vol. 44, pp. 1469-1480 (2006)

NEW DATA ON TYPE-LOCALITY SOROSITE: COMPOSITIONAL VARIATIONS, ZONING, AND A REVISED FORMULA

ANDREI Y. BARKOV[§], ROBERT F. MARTIN AND LANG SHI

Department of Earth and Planetary Sciences, McGill University, 3450 University Street, Montreal, Quebec H3A 2A7, Canada

ABSTRACT

We report new results of multiple EMP analyses of sorosite from the Baimka Au–PGE placer deposit, western Chukotka, northeastern Russia. It occurs as (1) relatively large (0.2–0.4 mm) euhedral, cryptically zoned hexagonal grains, with Fe–Ni-rich zones in the core, (2) large irregular or skeletal grains, and (3) elongate subhedral to euhedral (hexagonal), or anhedral micrograins (≤20 μm). They all are hosted by native tin (Sb-bearing), and are associated with stistaite $Sn_{1+x}Sb$ and herzenbergite SnS. The Fe content of these zoned grains decreases from the center (3 wt.%) toward the edge (≤0.05 wt.%). The Ni content also decreases from the core (1.2 wt.%) to the periphery (<0.02 wt.%). The level of Sb covaries positively with Fe and Ni; it is enriched in the core (5.8%) relative to the periphery (4%). The incorporation of Fe+Ni is thus somehow controlled by Sb. Values of 100 Fe / (Fe + Ni) also exhibit cryptic variations. On the basis of our results (214 EMP analyses acquired with three different instruments and sets of standards), the average composition of sorosite, recalculated for (Sn + Sb) = 1 *apfu*, is: $(Cu_{1.09–1.14}Fe_{0.02–0.05}Ni_{0.01–0.02})_{\Sigma 1.15–1.17}(Sn_{0.91–0.93}Sb_{0.07–0.09})_{\Sigma 1.00}$; the observed ranges are: Cu 0.97–1.19, Fe 0–0.13, Ni 0–0.04, Co <0.01, Σ*Me* 1.10–1.21, Sn 0.90–0.99, and Sb ≤0.01–0.10 *apfu*. The revised formula for sorosite is $(Cu,Fe)_{1+x}(Sn,Sb)$, where $0.1 \le x \le 0.2$. The excess Cu atoms (*i.e.*, 0.1–0.2 *Me apfu*), relative to CuSn, presumably occupy the trigonal-bipyramidal holes associated with interstitial sites of the NiAs-type lattice. The incorporation of Sb in sorosite is governed by two mechanisms of substitution: [Cu + Sn = (Fe+Ni) + Sb], consistent with the observed solid-solution of $Cu_{1+x}Sn$ (sorosite) with related NiAs-type antimonides: $Fe_{1+x}Sb$ (unnamed) and $Ni_{1+x}Sb$ (breithauptite), and by the Sb-for-Sn mechanism, which operates in Fe–Ni-poor sorosite. Sorosite likely crystallized from a late-stage or residual Sn–Sb–Cu–Fe–Ni-bearing liquid, under conditions of low $f(O_2)$ and $f(S_2)$; the inferred sequence of crystallization is: (1) large euhedral grains (Fe–Ni–Sb-rich core → Fe–Ni–Sb-poor periphery) → (2) large irregular grains (Fe–Ni-poor) → (3) various micrograins (Ni–Fe-poor, poorer in Sb than the large grains). Crystallization occurred over the range >415°–227°C, the latter being the eutectic temperature in the binary system Cu–Sn. A mineralized mafic rock (gabbro, gabbro–diorite, or clinopyroxenite) associated with the Yegdegkychsky gabbro – diorite – syenite – monzonite complex in the placer area could be a potential primary source for the sorosite-bearing mineralization.

Keywords: sorosite, $(Cu,Fe)_{1+x}(Sn,Sb)$, intermetallic compound, nickeline-type stannide, Cu–Sn system, Sn–Sb–Cu mineralization, cryptic zoning, solid-solution series, mechanisms of substitution, gold–PGE placer deposit, Baimka, Chukotka, Russia.

SOMMAIRE

Nous présentons les résultats de plusieurs nouvelles analyses (par microsondes électroniques) de la sorosite holotype, provenant du gisement d'or et d'éléments du groupe du platine de type placer de Baimka, partie occidentale de Chukotka, dans le nord-est de la Russie. La sorosite se présente (1) en grains idiomorphes (hexagonaux) relativement gros (0.2–0.4 mm) et cryptiquement zonés, avec enrichissement en Fe–Ni dans le noyau, (2) de gros grains irréguliers or skelettiques, et (3) des grains plutôt allongés, sub-idiomorphes ou idiomorphes, et des micrograins (≤20 μm) xénomorphes. Tous sont piégés dans l'étain natif contenant de l'antimoine, et ils sont associés à la stistaïte, $Sn_{1+x}Sb$, et la herzenbergite, SnS. La teneur en Fe de ces grains zonés diminue du centre (3%, poids) vers la bordure (≤0.05%). La teneur en Ni diminue aussi du coeur (1.2%) vers la bordure (<0.02%). Le niveau de Sb covarie positivement avec la teneur en Fe et Ni; il est enrichi dans le coeur (5.8%) par rapport à la bordure (4%). L'incorporation de Fe + Ni dépendrait donc de la teneur en Sb. Les valeurs de 100 Fe / (Fe + Ni) montrent aussi des variations cryptiques. D'après nos résultats (214 résultats d'analyses) acquis avec trois instruments différents et trois ensembles d'étalons, pour (Sn + Sb) égal à une atome par formule unitaire (*apfu*), la composition moyenne de la sorosite serait: $(Cu_{1.09–1.14}Fe_{0.02–0.05}Ni_{0.01–0.02})_{\Sigma 1.15–1.17}(Sn_{0.91–0.93}Sb_{0.07–0.09})_{\Sigma 1.00}$; les intervalles observés sont: Cu 0.97–1.19, Fe 0–0.13, Ni 0–0.04, Co <0.01, Σ*Me* 1.10–1.21, Sn 0.90–0.99, et Sb ≤0.01–0.10 *apfu*. La formule révisée de la sorosite est $(Cu,Fe)_{1+x}(Sn,Sb)$, dans laquelle $0.1 \le x \le 0.2$. L'excédent en atomes de Cu (*i.e.*, 0.1–0.2 *Me apfu*), par rapport à la stoechiométrie CuSn, occuperait les trous trigonaux-bipyramidaux associés aux sites interstitiels de la maille de type NiAs. L'incorporation de Sb dans la sorosite est régie par deux mécanismes de substitution: [Cu + Sn = (Fe+Ni) + Sb], ce qui concorde avec les compositions observées entre la solution solide $Cu_{1+x}Sn$ (sorosite) et les pôles semblables de type NiAs: $Fe_{1+x}Sb$ (sans nom) et $Ni_{1+x}Sb$ (breithauptite), et un

§ *E-mail address*: abarkov@eps.mcgill.ca

mécanisme de remplacement de Sn par Sb dans le cas de compositions à faible teneur en Fe–Ni. La sorosite aurait vraisemblablement cristallisé à partir d'un liquide tardif résiduel contenant Sn–Sb–Cu–Fe–Ni, à des conditions de faibles $f(O_2)$ et $f(S_2)$; la séquence de cristallisation serait: (1) gros grains idiomorphes enrichis en Fe–Ni–Sb dans le coeur et diminuant vers la bordure → (2) gros grains irréguliers (à faible teneur en Fe–Ni) → (3) micrograins (à faible teneur en Ni–Fe, et encore plus faibles en Sb que les gros grains). La crystallisation a eu lieu sur l'intervalle >415°–227°C, cette dernière la température du point eutectique dans le système binaire Cu–Sn. Une roche mafique minéralisée (gabbro, gabbro–diorite, ou clinopyroxénite) associée au massif de gabbro – diorite – syénite – monzonite de Yegdegkychsky, dans la région du placer, pourrait s'avérer la source primaire de la minéralisation porteuse de sorosite.

(Traduit par la Rédaction)

Mots-clés: sorosite, $(Cu,Fe)_{1+x}(Sn,Sb)$, composé intermétallique, stannure de type nickeline, système Cu–Sn, minéralisation Sn–Sb–Cu, zonation cryptique, solution solide, mécanismes de substitution, gisement d'or et d'éléments du groupe du platine, Baimka, Chukotka, Russie.

Introduction

Sorosite, an intermetallic mineral of Cu and Sn with a composition close to Cu(Sn,Sb) and a hexagonal structure close to that of nickeline, NiAs, was discovered in association with Pt–Fe alloy minerals and gold in the Baimka placer deposit, northeastern Russia (Barkov *et al*. 1998). Recently, we have conducted multiple wavelength-dispersion electron-microprobe analyses (WDS EMP) of sorosite grains from the Baimka deposit. Our objectives in this study are: (1) to report results of new EMP analyses and to characterize compositional variations, extents of element substitutions and mechanisms controlling the incorporation of elements other than Cu and Sn in the type-locality sorosite, (2) to compare the composition of texturally distinct generations of sorosite grains, (3) to document the existence of a cryptic zoning, (4) to suggest a revision of the Cu(Sn,Sb) formula, (5) to make a comparison with various NiAs-type phases related to sorosite, and (6) to discuss aspects of the crystallization history of sorosite and its potential primary source-rocks.

Geological Background

Two large magmatic complexes are known in the vicinity of the Baimka Au–PGE placer deposit associated with the Baimka River (near the River Bol'shoy Anyuy) and located in the Aluchin horst, western Chukotka, northeastern Russia. (1) The Aluchin ophiolite complex, of Permian or Triassic age, roughly ~250 km^2 in area, consists mainly of harzburgite, subordinate dunite, both serpentinized to various degrees, and pyroxenite, with abundant dikes of olivine dolerite, trachydolerite, diorite porphyry, aplite and numerous quartz veins along the contact (Dovgal 1964, Aksenova *et al*. 1970, Lychagin 1985, Surnin & Okrugin 1989). Occurrences of chromite and Ni–(Fe) sulfide mineralization are associated with the Aluchin complex (Aksenova *et al*. 1970). (2) The Yegdegkychsky (or Yegdegkychskii) gabbro – diorite – (monzonite) – syenite complex of Jurassic (to Cretaceous?) age is a result of two or three intrusive phases: an early gabbro and gabbro–diorite phase, and later phases of various syenites, quartz-bearing and of alkaline affinity, and quartz-bearing diorites (Berlimble & Gorodinskii 1978, Gorodinskii *et al*. 1982, Volchkov *et al*. 1982). In addition, zoned clinopyroxenite–gabbro intrusions up to ~4.5 km in diameter are present; they seem to belong to an early intrusive sequence of the Yegdegkychsky complex. These intrusions are likely related to Uralian–Alaskan-type complexes and probably represent the primary source for placer platinum-group minerals (PGM) in the Baimka deposit (Gornostayev *et al*. 1999). Also, various subvolcanic bodies and associated hornfelsic rocks are developed in this area (Gulevich 1974, Gorodinskii *et al*. 1982). The porphyry-copper, Au–Ag-bearing polysulfide ores, and (quartz)–Mo–Cu–(Au) mineralization are associated with quartz-bearing monzonite porphyry and related hypabyssal rocks of the Yegdegkychsky complex, which is probably the principal source of gold placer deposits in this region (Gulevich 1974, Berlimble & Gorodinskii 1978, Volchkov *et al*. 1982, Kaminskii 1987, 1989).

Association and Texture

Sorosite has been found in a few placer grains 3–4 mm across that are principally composed of native tin (Sb-bearing); these grains were recovered along with Pt–Fe alloy and gold in the Baimka deposit. The relative abundance of sorosite is somewhat higher than that of the associated stistaite, a rarely encountered antimonide of formula $Sn_{1+x}Sb$ ($Sn_{1.12–1.13}Sb_{0.87–0.88}$), which forms lath-shaped crystals up to 0.3 mm long. Minor amounts of herzenbergite (SnS), moissanite(?), native lead, cassiterite, troilite, djerfisherite, and titanian magnetite were observed as minute inclusions in native tin. Individual grains of sorosite of distinctive morphology and size, and mutual intergrowths with stistaite, are hosted by native tin.

Various textural forms of sorosite are observed: (1) large euhedral, hexagonal grains (0.2–0.4 mm) with well-developed faces (Fig. 1A), which typically contain Fe–Ni-enriched zones in the core, as documented below, (2) large irregular or partly skeletal grains, and (3) micrograins (≤20–30 μm in size), which are commonly

elongate, subhedral to euhedral (also well-developed hexagonal: Fig. 1B) or anhedral, and aggregates of such micrograins. Larger grains of sorosite are commonly and extensively fragmented and fractured (in polished mount), consistent with microhardness measurements indicating that sorosite is hard and brittle. However, these fractures may represent a primary feature, probably related to a change in volume during crystallization and cooling.

Results: Cryptic Zoning in Sorosite

The relatively large euhedral grains of sorosite typically are zoned with respect to the minor elements Fe, Ni, and Sb. In all cases, levels of Co are close to the minimum limit of detection (EMP), and we thus could not evaluate its distribution. This cryptic zoning is not observed optically; we document its presence in high-contrast back-scattered-electron images, element-distribution maps (Figs. 2A,B), and detailed EMP

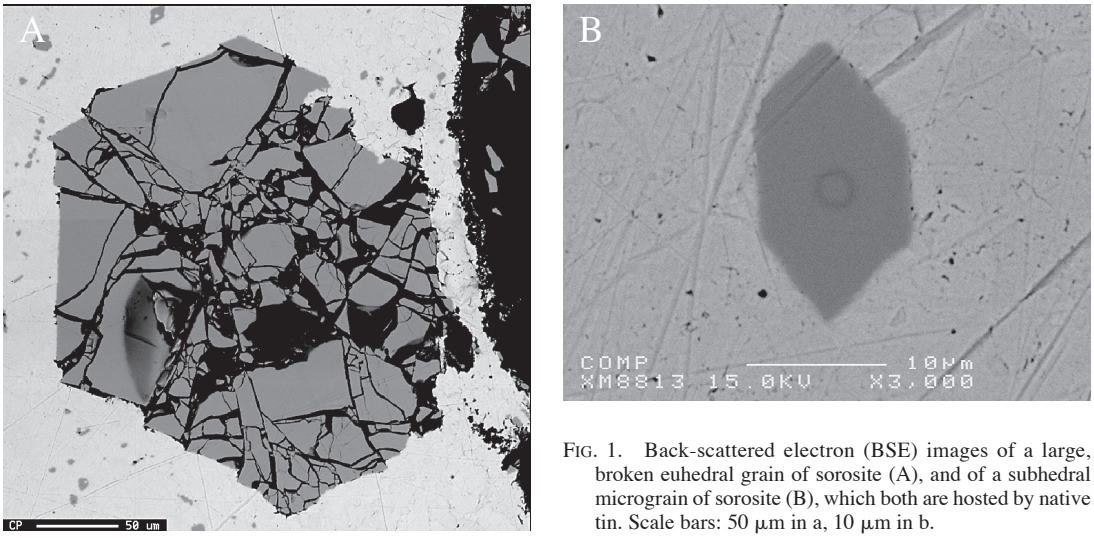

FIG. 1. Back-scattered electron (BSE) images of a large, broken euhedral grain of sorosite (A), and of a subhedral micrograin of sorosite (B), which both are hosted by native tin. Scale bars: 50 μm in a, 10 μm in b.

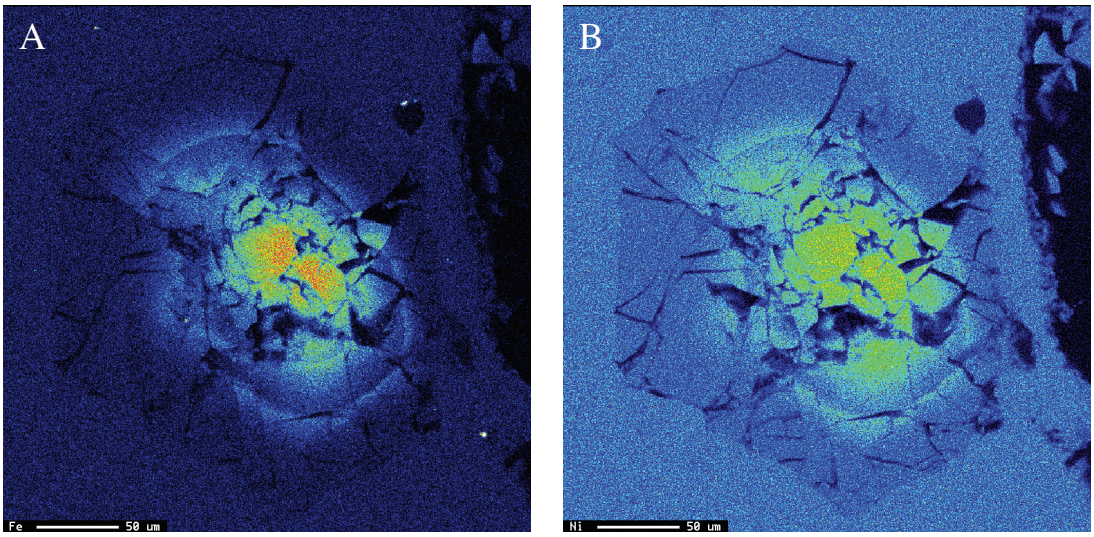

FIG. 2. Color X-ray maps showing the distribution of Fe (A) and Ni (B) in the cryptically zoned grain of sorosite shown in Figure 1A.

profiles, such as those obtained for two representative crystals, labeled Crystals 1 and 2 (Figs. 3A–E). The Fe content of these crystals gradually decreases from the center (up to about 3 wt.%) toward the edge, where sorosite becomes virtually devoid of Fe (≤0.05 wt.%; Fig. 3A). The level of Ni invariably is lower than that of Fe; it reaches its maximum in the core (up to 1.2 wt.%: Fig. 3B), in parallel with Fe, and then gradually decreases outward (<0.02 wt.% Ni at the edge). In contrast, the level of Cu is relatively low at the center (Fig. 3C) and varies antipathetically with Fe + Ni, indicative of a (Fe + Ni)-for-Cu substitution. Antimony, which substitutes for Sn in sorosite, covaries positively with Fe and Ni, and also shows enrichment in the core (up to 5.8 wt.% Sb), relative to the periphery (about 4 wt.% Sb), and decreases smoothly outward (Fig. 3D). These compositional trends suggest that the incorporation of Fe + Ni is somehow controlled by Sb. Note, however, that, the Ni–Fe-poor zones, developed at the edge of sorosite grains, are Sb-bearing (Fig. 3D), so that the incorporation of substantial Sb in sorosite is not necessarily controlled by Fe and Ni.

Interestingly, results of our EMP analyses suggest that values of the atom ratio 100 Fe / (Fe + Ni) also exhibit cryptic variations in the zoned grains; however, compositional trends observed for the Crystals 1 and 2 are somewhat distinct. In Crystal 1, values of this ratio generally decrease toward the edge (Fig. 3E), thus indicating that Fe is partitioned more strongly than Ni into the core in this crystal. The trend shown by Crystal 2 is more complex. Values of 100 Fe / (Fe + Ni) reach a maximum in the center of Crystal 2, and decrease outward; then, closer to the periphery, the observed trend bends rapidly, with a marked increase toward the edges (Fig. 3E). These variations could be a reflection of sudden change in the environment or conditions of crystallization, *e.g.*, a rise in the activity of Fe with a corresponding increase in Fe:Ni ratio in the residual melt.

Compositional Variations and Element-Correlation Relationships

Previously, sorosite was considered to be relatively homogeneous in composition (Barkov *et al.* 1998). However, we note that the total content of base metals (Cu + Fe + Ni + trace amounts of Co) ranges from 1.10 to 1.21 atoms per formula unit, *apfu*, in the entire set of our EMP analyses (Fig. 3F), including 214 point analyses (WDS: n = 214), made on various euhedral and irregular large grains, as well as representative micrograins. The EMP data, plotted in Figure 3F, were recalculated on the basis of (Sn + Sb) = 1 *apfu*. The level of Fe correlates strongly positively with that of Ni; the correlation coefficient R is 0.94, calculated for n = 212 (large grains only) on the basis of a total of 2 *apfu*, corresponding to an idealized NiAs-type formula (Fig. 4A). The Fe *versus* Sb and the Ni *versus* Sb correlations, observed in compositions of the large grains (*LG*: Figs. 4B, C), are strong and positive, with R equal to 0.94 and 0.84, respectively (for n = 212). Note that compositions of two micrograins of sorosite (*MG*) plotted in Figures 4B and 4C are representative of the micrograin generation, and they are in good agreement with multiple analyses of micrograins of sorosite from Baimka (Barkov, unpubl. results of SEM–EDS analyses). The micrograins are very poor in Sb (0.01–0.02 *apfu*) and are virtually devoid of Fe and Ni (Figs. 4B, C); they are notably distinct in composition from the large grains of sorosite. In addition, these micrograins plot off the linear compositional trend observed for the large grains, which indicate the existence of a strongly positive correlation of Sb *versus* Fe + Ni (R = 0.92 for n = 212: Fig. 4D).

The amount of Cu is inversely correlated with Fe + Ni (R = –0.98: Fig. 4E). Note that if calculated on the basis of Σatoms = 2 *apfu*, assuming an ideal NiAs-type formula, the Cu content of Fe–Ni-poor (or -free) sorosite exceeds 1 *apfu* and varies in the range 1.05–1.1 *apfu* (Fig. 4E). The existing deviation from the ideal (1:1) proportions is also displayed in Figure 4F, in a plot (Cu + Fe + Ni + Co) *versus* (Sn + Sb). The observed range of composition, $(Cu,Fe,Ni,Co)_{1.05–1.1}(Sn,Sb)_{0.9–0.95}$, based on Σatoms = 2 *apfu*, reveals the existence of excess amounts of these base metals (relative to CuSn). The degree of this excess is better characterized by atom proportions based on (Sn + Sb) = 1 *apfu*; this basis of recalculation is in agreement with formulae of related NiAs-type compounds, and is thus preferred for sorosite.

On the basis of (Sn + Sb) = 1 *apfu*, the average composition of the type-locality sorosite, obtained using different facilities (WDS EMP), is: $(Cu_{1.09–1.14}Fe_{0.02–0.05}Ni_{0.01–0.02})_{\Sigma 1.15–1.17}(Sn_{0.91–0.93}Sb_{0.07–0.09})_{\Sigma 1.00}$ (Table 1), and the observed compositional ranges (for n = 214) are: Cu 0.97–1.19, Fe 0–0.13, Ni 0–0.04, Co <0.01, Σ*Me* 1.10–1.21 (Fig. 3F), Sn 0.90–0.99, and Sb ≤0.01–0.10 *apfu*.

Discussion

Intermetallic compounds related to sorosite: comparison and implications

Results of an X-ray powder-diffraction study (Barkov *et al.* 1998) indicate that sorosite from the Baimka deposit has a NiAs-type structure, with a 4.217, c 5.120 Å, and is isostructural with the η-phase ("Cu_6Sn_5" with a 4.190 and c 5.086 Å: PDF 2–0713), which appears at about 60 wt.% Sn in the Cu–Sn system at lower temperatures (Westgren & Phragmén 1928). In "Cu_6Sn_5" (*i.e.*, $Cu_{1+x}Sn$), the Cu atoms in excess of CuSn (*i.e.*, about 0.2 *apfu*) are statistically distributed within the interstices of the lattice. Sorosite is related to the numerous members of the nickeline group, which includes various antimonides, arsenides, bismuthides,

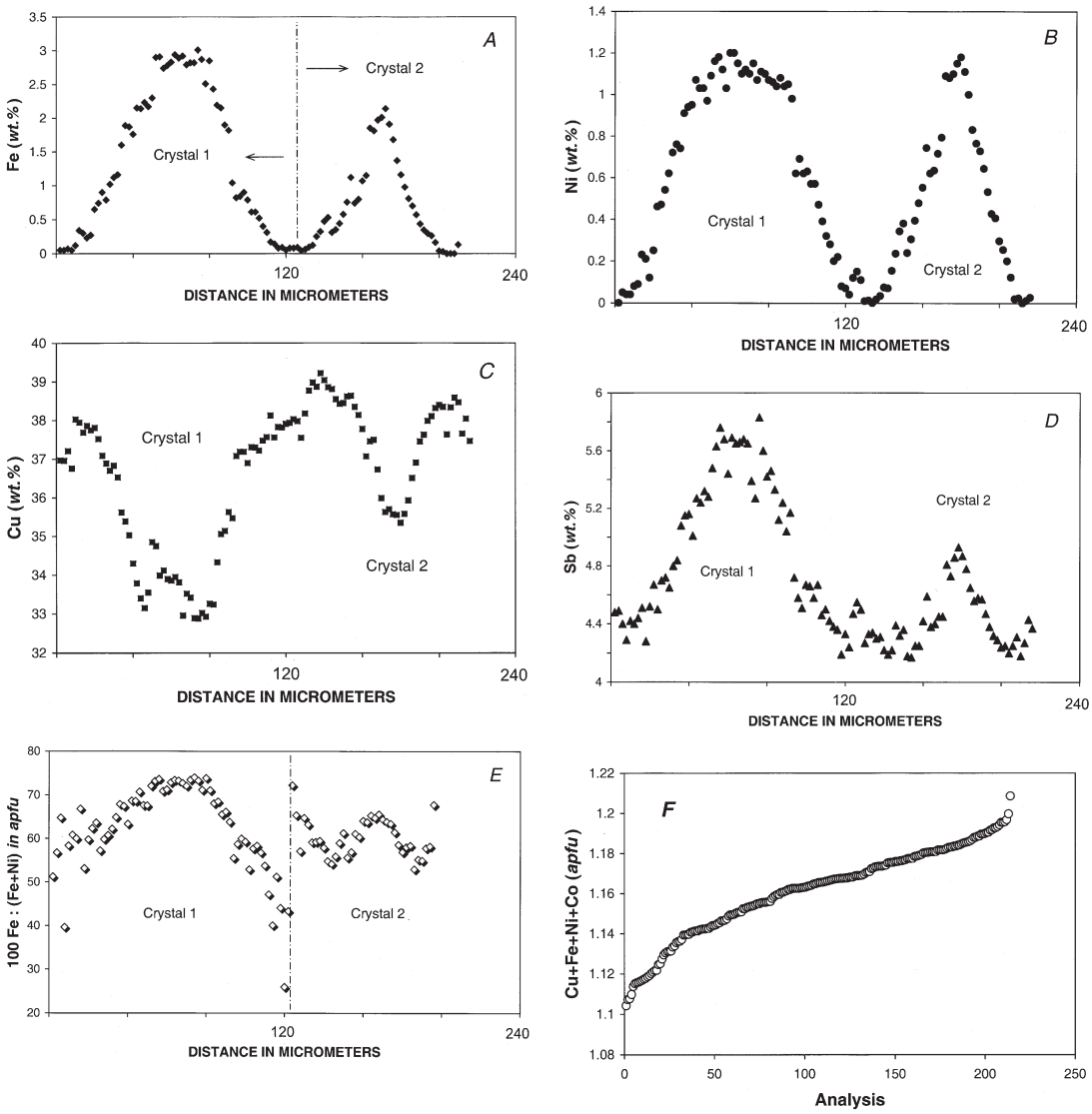

FIG. 3. Variations in content of Fe (Fig. 3A), Ni (B), Cu (C), and Sb (D), expressed in wt.%, and values of the atom ratio 100 Fe / (Fe + Ni) (Fig. 3E) along electron-microprobe profiles and across two zoned grains of sorosite (*i.e.*, "Crystal 1" and "Crystal 2"). Figure 3F shows variations in the total content of metals, observed in this study for sorosite in terms of (Cu + Fe + Ni + Co), expressed in atoms per formula unit, *apfu* (basis: Sn + Sb = 1 *apfu*). Results of a total of two hundred and fourteen WDS analyses are plotted in the order of increasing ΣMe value (Fig. 3F).

selenides, stannides and tellurides of idealized formula *AX*, where *A* is Co, Ni, Pd, or Pt, and *X* is As, Bi, Sb, Se, Sn, or Te.

It should be emphasized that NiAs-type compounds commonly display considerable deviations from the *AX* formula, and are rather consistent with the $A_{1+x}X$ formula, which is also indicated for sorosite (Table 1). Synthetic NiAs-type antimonides, $Fe_{1+x}Sb$, $Cr_{1+x}Sb$, $Co_{1+x}Sb$, $Ni_{1+x}Sb$, $Pd_{1+x}Sb$, and $Pt_{1+x}Sb$, also are consistent with this formula, values of x in which may be positive, negative, or equal 0 (Kjekshus & Walseth 1969). Two of these phases, $Fe_{1+x}Sb$ and $Ni_{1+x}Sb$, are especially relevant, because of the strongly positive Fe *versus* Sb and Ni *versus* Sb correlations observed in sorosite (Figs. 4B, C). Extensions of the homogeneity ranges are temperature-dependent for all of these

synthetic phases (Kjekshus & Walseth 1969). The excess atoms of metal occupy interstitial positions in the various NiAs-type compounds, *e.g.*, the excess Fe atoms in synthetic $Fe_{1+x}Sb$ with $0.08 \le x \le 0.38$ (Yamaguchi *et al.* 1972), $0.08 \le x \le 0.64$ (Yashiro *et al.* 1973), and $0.13 \le x \le 0.30$ (Richter & Schmidt 1975). Lefevre *et al.* (1978) reported a "Fe_7Sb_6" ($Fe_{1.17}Sb$) composition for the $Fe_{1+x}Sb$ phase. Interestingly, the Fe:Sb proportion in synthetic $Fe_{1.17}Sb$ is identical to that observed in an average composition of sorosite, with the (Cu + Fe + Ni):(Sn + Sb) ratio of 1.17 (anal. 1, Table 1). Nonstoichiometry existing in synthetic $Ni_{1+x}Sb$, which also has a B_8 (NiAs) structure, is a result of a defect mechanism: Ni atoms first occupy octahedral sites, and before these sites are completely filled, Ni atoms start to fill the trigonal-bipyramidal holes (*i.e.*, interstitial sites) of the NiAs lattice (Leubolt *et al.* 1986).

The Ni–Sb and Fe–Sb correlations (Figs. 4B, C) indicate the existence of solid-solution series extending from $Cu_{1+x}Sn$ (sorosite) toward $Fe_{1+x}Sb$ (unnamed) and $Ni_{1+x}Sb$ (breithauptite). These series are clearly promoted by the fact that $Fe_{1+x}Sb$ and $Ni_{1+x}Sb$ are isotypic with sorosite. Corresponding monostannides of Fe and Ni having a NiAs-type structure are unknown. Previously, a "$Ni_{1.5}Sn$" phase was reported as a representative of the NiAs family (Wever & Wintermann 1961); however, the structure of NiSn is orthorhombic, and results from the removal of Ni-chains from a defect NiAs structure (Bhargava & Schubert 1973). Note that yuanjiangite, AuSn, does have the NiAs-type structure; it was discovered in sandy gravels rich in placer gold, in a moraine-type glaciofluvial deposit, China (Chen *et al.* 1994).

The NiAs-type phases readily form mutual solid-solutions, *e.g.*, continuous series exist between NiAs-type phases in the systems Fe–Sb and Co–Sb (Geller 1939), the systems Ni–Sb and Fe–Sb (Ageev & Makarov 1943), and in the following systems: $(Fe_{1.2}Sb)_{1-x}(Ni_{1.2}Sb)$ with $0 < x < 1.0$, $(Fe_{1.2}Sb)_{1-x}(NiSb)_x$ with $x = 0.4$ and 0.6, $(Fe_{1.2}Sb)_{1-x}(CoSb)_x$ with $x = 0.25$ and 0.75, and $(CoSb)_{1-x}(NiSb)_x$ with $0.15 < x < 0.85$ (Gal'perina *et al* 1977). The last-named compounds have a NiAs-type structure consisting of a hexagonal close-packed sublattice with the transition-metal atoms localized in octahedral voids to form a cation sublattice, whereas trigonal-bipyramidal voids associated with tetrahedral interstices accommodate the excess atoms (Gal'perina *et al* 1977). Naturally occurring members of the nickeline group also display mutual solid-solutions, *e.g.*, between nickeline (NiAs) and breithauptite (NiSb) in mineralized cavities of dolomite veins in the Belorechensk deposit, northern Caucasus (Pekov 1993).

The Sb content of sorosite is up to 0.1 *apfu* in the Baimka deposit. Greater amounts of Sb could probably be incorporated in sorosite, depending on conditions of crystallization; however, a Sb-for-Sn substitution appears to be somewhat limited in this species, and coupled substitutions involving Sb and Sn could be more extensive. A ternary "$Cu_{12}Sb_3Sn_7$" phase, reported in the system Cu–Sn–Sb (Tasaki 1929), corresponds to $Cu_{1.2}(Sn_{0.7}Sb_{0.3})$, and thus is conformable in atom proportions with $Cu_{1.2}Sn$ (η-Cu_6Sn_5), *i.e.*, the synthetic equivalent of sorosite. Therefore, up to 0.3 Sb *apfu* could probably be incorporated in sorosite *via* a simple Sb-for-Sn substitution.

Interestingly, Larsson *et al.* (1994) reported the existence of domain-twinning in synthetic η'-Cu_6Sn_5, leading to a new type of superstructure (space group C_2/c), belonging to the NiAs–Ni_2In structure group. They noted that macroscopically, this domain-twinning gives rise to perfect hexagonal symmetry, thus explaining the hexagonal cell suggested for η-Cu_6Sn_5. It remains unknown, however, if a superstructure exists in sorosite. In addition, structural modulations

TABLE 1. AVERAGE RESULTS OF ELECTRON-MICROPROBE ANALYSES OF SOROSITE FROM THE BAIMKA Au–PGE PLACER DEPOSIT, RUSSIA

	1	2	3
n	50	151	10
Cu wt.%	37.58	35.96	35.97
Fe	0.69	1.26	1.47
Ni	0.44	0.64	0.59
Co	n.d.	n.d.	0.02
Sn	57.51	56.78	56.43
Sb	4.30	4.89	5.23
Total	100.52	99.53	99.71
Composition based on Σatoms = 2 *apfu*			
Cu *apfu*	1.05	1.01	1.01
Fe	0.02	0.04	0.05
Ni	0.01	0.02	0.02
Co	–	–	<0.01
Σ*Me*	1.08	1.07	1.08
Sn	0.86	0.86	0.85
Sb	0.06	0.07	0.08
Sn + Sb	0.92	0.93	0.93
Compositions based on (Sn + Sb) = 1 *apfu*			
Cu	1.14	1.09	1.09
Fe	0.02	0.04	0.05
Ni	0.01	0.02	0.02
Co	–	–	<0.01
Σ*Me*	1.17	1.15	1.16
Sn	0.93	0.92	0.92
Sb	0.07	0.08	0.06
Sn + Sb	1	1	1
Σ*Me* / (Sn + Sb)	1.17	1.15	1.16

The results of the wavelength-dispersion EMP analyses that led to the average composition no. 1 were acquired with a JEOL JXA–8900 instrument (20 kV and 30 nA), using the following X-ray lines and standards: Cu*Kα* ($CuFeS_2$), Fe*Kα* (FeS_2), Ni*Kα* [CoNiAs], Sn*Lα* (SnO_2), and Sb*Lα* (Sb_2S_3). The analyses that led to the average compositions no. 2 and 3 were carried out with a JEOL–733 and a Cameca SX–50 instrument, respectively. A finely focused beam (≤2 μm) was applied in all cases; *n* is the number of individual analyses. The grains were analyzed for Pd, Pt, Au, As, Se, Bi, Te, and S, but these elements were not detected. Atoms per formula unit: *apfu*.

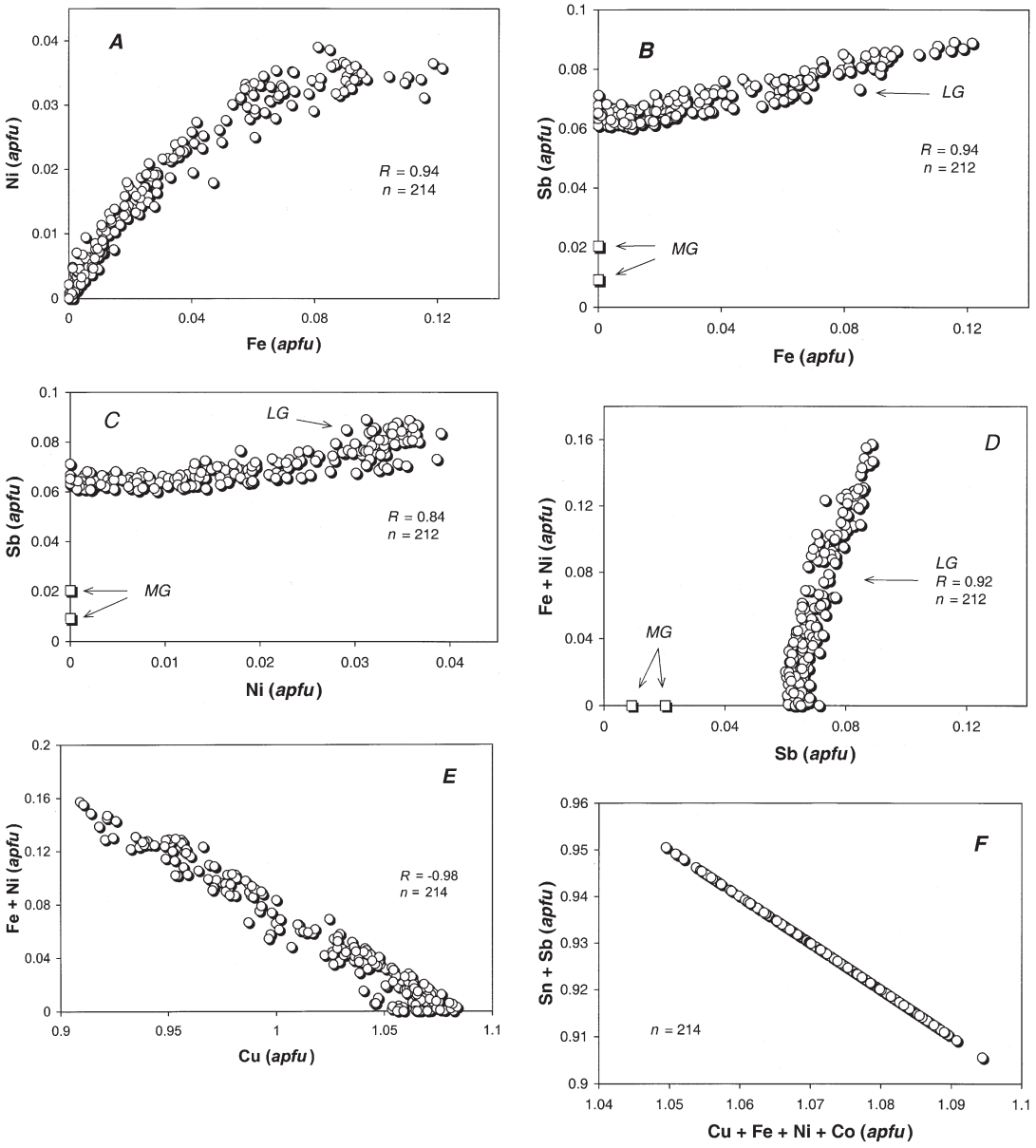

FIG. 4. Compositional variation of sorosite in terms of the plot of Fe *versus* Ni, expressed in *apfu* on the basis of Σatoms = 2 *apfu* (Fig. 4A), Fe *versus* Sb (B), Ni *versus* Sb (C), (Fe + Ni) *versus* Sb (D), (Fe + Ni) *versus* Cu (E) and (Cu + Fe + Ni + Co) *versus* (Sn + Sb) (F). Results of two hundred and twelve WDS analyses of large grains of sorosite (*LG*: circles) and representative compositions of two micrograins of sorosite (*MG*: squares) are plotted.

were reported in a high-temperature modification of η-Cu_6Sn_5, *i.e.*, reassigned η-Cu_5Sn_4, showing two superstructures (C_2 and P_21/c), caused by the ordered occupancy of Cu in the trigonal-bipyramidal sites (Larsson *et al.* 1995). The sorosite at Baimka differs slightly in atom proportions from η-Cu_5Sn_4; the *Me*:(Sn+Sb) ratio of sorosite is 1.1–1.2, compared to 1.25 in η-Cu_5Sn_4.

Revised formula and mechanisms of substitution in sorosite

Our EMP data, presented in Figures 3F and 4A–F, suggest the following revision of the formula for sorosite: $(Cu,Fe)_{1+x}(Sn,Sb)$, where $0.1 \leq x \leq 0.2$. This revision is consistent with the successful synthesis of $Fe_{1+x}Sb$ and $Ni_{1+x}Sb$ (equivalent of breithauptite) (*e.g.*, Lefevre *et al.* 1978, Leubolt *et al.* 1986), which are of NiAs type, and very closely related to sorosite. As is inferred from the revised formula, and by analogy with the related phases, the excess Cu atoms, relative to CuSn, likely occupy the trigonal-bipyramidal holes associated with interstitial sites of the NiAs-type lattice.

On the basis of these results (Figs. 4A–F), we also infer that two mechanisms of substitution control the incorporation of Sb in sorosite: (1) the coupled substitution [Cu + Sn = (Fe + Ni) + Sb] is a result of solid-solution series extending from $Cu_{1+x}Sn$ toward $Fe_{1+x}Sb$ and $Ni_{1+x}Sb$. (2) The second mechanism, Sb-for-Sn, operates in sorosite poor in Fe and Ni (Figs. 4B–D).

Generations of sorosite and crystallization history

The textural and compositional data obtained in this study are consistent with three main stages of crystallization of sorosite in the Baimka deposit. At stage 1, large euhedral and zoned grains of sorosite crystallized from a late-stage or residual Sn–Sb–Cu–Fe–Ni-bearing melt under conditions of low $f(O_2)$ and $f(S_2)$. These zoned grains crystallized from a Fe–Ni-rich core to a Fe–Ni-poor periphery (Figs. 3A–E), during a normal decrease in temperature in the system. At stage 2, the large irregular or skeletal grains of sorosite (also Fe–Ni-poor) crystallized nearly simultaneously with the Fe–Ni-poor periphery zones of the zoned crystals. Finally, at stage 3, the abundant micrograins of sorosite formed from the host native tin. These micrograins are poor in Ni and Fe, and are poorer in Sb than the associated coarse grains (Figs. 4B–D). Thus, we infer that levels of Sb, Fe, and Ni in sorosite generally decreased with decreasing temperature, and that higher temperatures of crystallization likely promoted the incorporation of these components in the structure.

The phase diagram for the system Cu–Sn (Saunders & Miodownik 1990, Fig. 1) allows us to be more specific about the temperature of formation of sorosite. In that binary system, the analog of sorosite, phase η, with 59 wt.% Sn, has a field of stability below 415°C. It crystallizes over the interval 415°–227°C from a tin-rich melt, the latter temperature being that of the eutectic reaction L → phase η + Sn. The presence of small amounts of Fe, Ni and Sb in our system is expected to raise the upper stability of sorosite, but these elements are removed from the residual melt efficiently by fractional crystallization. The micrograins of sorosite embedded in native tin in our stage-3 generation presumably represent a recrystallized eutectic assemblage, thus formed very close to 227°C.

Potential primary source-rocks for sorosite

In Table 2, we have summarized occurrences of native tin and intermetallic compounds of Sn and Cu, reported in the literature from various localities. As can be seen from this listing, a wide spectrum of mineralized rock-types could in principle produce sorosite-bearing placer mineralization. However, the geological background of the Baimka placer area and the association with Pt–Fe alloy minerals suggest a provenance from an ophiolitic or Uralian–(Alaskan–Aldan)-type complex, namely, the Aluchin ophiolite complex or the Yegdegkychsky gabbro – diorite – monzonite – syenite complex and related concentrically zoned clinopyroxenite–gabbro intrusions. The low values of $f(O_2)$ and $f(S_2)$ required for the formation of the sorosite-bearing (Sn–Sb–Cu–Fe–Ni–Pb) mineralization were achieved at a very late stage of crystallization in an ophiolitic or Uralian-type complex. The provenance from a mineralized zone associated with the Yegdegkychsky complex appears more probable, however. This suggestion is consistent with a primary Uralian-type source inferred for the placer PGM in the Baimka deposit (Gornostayev *et al.* 1999), and with the presence of micro-inclusions of djerfisherite and titanian magnetite in native tin at Baimka. The Uralian- and related Aldan-type complexes are known to be associated with various alkaline rocks, and a genetic relationship with such a complex would explain the enrichment in Sb characteristic of the sorosite-bearing assemblage of minerals. For example, aggregates of native Sb and Pb, Cu–Sb phases and intergrowths of Pb–Sb phases (with PGM inclusions) and clinopyroxene occur in a PGM–Au placer deposit derived from an Aldan-type alkaline mafic–ultramafic body, central Aldan region, Russia (Kim & Leskova 1988). Interestingly, anyuiite, $AuPb_2$, a very rare species containing up to 0.29 Sb *apfu*, had been discovered in PGM–Au-bearing placers of the Anyuy River in the same general area. In these placers, anyuiite occurs as intergrowths with native Pb and Au, in association with titanian magnetite and Cr-rich members of the spinel group, which may well imply a Uralian-type provenance (Razin & Sidorenko 1989). On the other hand, the strong enrichment in Sn (and Cu) in sorosite could be rather typical of a mafic rock, *e.g.*, trap rocks in Siberian Platform, Russia, which host a similar mineralization of native Sn, Cu–Sn alloy (natural "bronze") and stistaite, associated with a diverse assemblage of native Fe, Cu (Ni-rich), Zn, Pb, Cd, Al and Mg_2Si (Okrugin *et al.* 1981), or the Noril'sk complex, Siberia, in which Pd–Pt–Cu stannides of the taimyrite–tatyanaite series are abundant (Barkov *et al.* 2000a, b). In summary, therefore, a mineralized mafic rock (gabbro, gabbro–diorite, or clinopyroxenite) in the

TABLE 2. WORLDWIDE OCCURRENCES OF NATIVE TIN AND INTERMETALLIC COMPOUNDS OF Sn AND Cu

Mineral or phase	Locality; host rock; associated minerals	Reference
Sorosite, native Sn	Mid-Atlantic Ridge (Mir zone); sediments	Dekov *et al.* (2001)
Sn–Cu alloy (Ag-bearing "bronze")	Ferromanganese oceanic (Mid-Pacific) crust; native Fe, Ni, Cu, Pb; alloys of Fe–Mn, Fe–Cr–Ni, Fe–Cr–Ni–Si, Fe–Co–Ni–Al–Cu; silicides of Cu–Pt and Fe, rustenburgite [$(Pt,Pd)_3Sn$], *etc.*	Rudashevskii *et al.* (2001)
Cu–Sn–(Pb) alloy ("bronze")	Glasberget pegmatite, Sweden; "asphaltite" spheroids with inclusions of native Fe, Ni, Cu (Ni–Zn-rich), NbBi, *etc.*	Yushkin *et al.* (2000)
Native Sn	Osinovka–Abramovka River area, Primor'ye, Russia; kaolinized carbonaceous-siliceous shales, intruded by hydrothermally altered basic dikes; native Pb, Fe, Ta	Seredin *et al.* (1998)
Native Sn	Western slope of the South Urals, Russia; complexly deformed carbonaceous sedimentary rocks ("black shale" complex) with Au–PGE mineralization.	Kovalev *et al.* (1997)
Native Sn	Northern Baikal region, Russia; Sukhoi Log Au–Ag–Pt deposit, associated with metasedimentary rocks ("black schists") enriched in organic matter; native Au, Ag, Pt, Fe, Cr, Al, Ti, W, Pb, Cu, and sulfides of Fe	Laverov *et al.* (1997)
Native Sn	Ozernaya River, Kamchatka, Russia; porous pumice in a volcanic bomb of rhyolite–dacite; magnetite, native Fe, Cu, graphite, metamorphosed organic matter.	Shterenberg (1997)
Native Sn, Cu_6Sn_5	Kubaka Au–quartz–orthoclase (adularia) deposit, Omolon massif, Okhotsk–Chukotka volcanogenic belt, northeastern Russia; stistaite and various intermetallic compounds with (Sn+Pb):Sb ratios of 2:1, 3:2, 4:3, *etc.*	Krivitskaya *et al.* (1995)
Cu–Sn phases	Mid-Atlantic Ridge (central part); magmatic rocks (gabbro, dolerite, basalt); native Fe, Cu (Zn-rich)	Akimtsev (1992)
Native Sn+Pb (intergrowths)	Exhalation products of fissure eruption, Bolshoi Tolbachik volcano, Kamchatka, Russia; native Fe, Al, Cu (Zn-rich) in interstices of basaltic scoria	Glavatskikh (1990)
Native Sn	Skarns, formed under influence of granite, Gåsborn area, west Bergslagen, central Sweden; W–Mo polymetallic mineralization, native Pb	Damman & Kieft (1990)
Sn–Pb phase	Central Aldan, Siberian Platform; lamproite; native Cu (Zn-rich), Zn, Fe (Cr-rich), Al	Eremeev *et al.* (1988)
Native Sn	Elgygytgyn meteorite crater, Chukotka, Russia; impactites, glassy bombs, shock-metamorphosed volcanic rocks; native Pb, Zn	Gurov & Kudinova (1987)
Native Sn	Ultramafic complexes, Koryak Upland, Russia; dunite, harzburgite, orthopyroxenite, websterite, gabbro-norite; metallic spheroids (native Fe, Cu, Cr, Al, Pb, Cu–Zn phases, W–Ti carbides) with a porous rim containing olivine, orthopyroxene, wüstite, armalcolite, ulvöspinel, ilmenite	Rudashevskii *et al.* (1987)
Native Sn+Pb	Cape Verde Islands; Miocene carbonatites associated with subaerial volcanic and subvolcanic facies; native Cu (Zn-rich), Fe, Ti	Frikh-Khar *et al.* (1986)
Native Sn+Pb	Western Liaoning province, China; volcanic tuff	Liu & Wang (1986)
Native Sn, Cu_6Sn_5, stistaite (Pb-rich), Cu_3Sn	Leningrad pipe, western Ukukitskoe field, Russia; autolithic kimberlite breccia. Native Cu (Zn-rich), Pb, Zn, Al, graphite, cuprostibite, CuZn	Koval'skii & Oleinikov (1985)
Cu–Sn alloys	Alluvial deposits, Sumatra, Kalimantan, Indonesia, East Malaysia; native Au, Pt, Cu–Au alloys, Os–Ir alloys	Bowles (1984)
Native Sn	Kumaksh ore field, Tajikistan; quartz veins, quartz–carbonate–feldspar metasomatic rocks; native Al, Fe, Cu, Zn, Pb, intermetallic compounds of Pb, Sn, Sb and of Cu, Pb, Sn, Sb	Novgorodova (1983)
Native Sn	Southern Sikhote–Alin, Russia; orogenic volcanic rocks (potassic rhyolites, shoshonitic andesites); native Pb, Cu, Zn, moissanite	Filimonova *et al.* (1981)
Native Sn, Cu–Sn alloy ("bronze")	Siberian Platform, Russia; trap rocks; native Fe, Cu (Ni-rich), Zn, Pb, Cd, Al, stistaite, Mg_2Si, Al_2CuMg, *etc.*	Okrugin *et al.* (1981)
Native Sn, Cu_6Sn_5 (Sb-rich)	Rio Tamana Choco district, Colombia; Au–Ag alloy, stistaite	Rose (1981)
Cu_6Sn_5	Panasqueira mine, Portugal; oxidized Sn ores	Clark (1972)
Native Sn, Cu(Sn,Sb), stistaite	Elkiaidai Brook, northern Nura–Tau Ridge, Uzbekistan	Nikolaeva *et al.* (1970)

Yegdegkychsky gabbro – diorite – monzonite – syenite complex would appear to be a likely primary source for the sorosite-bearing mineralization.

Conclusions

(1) The following average composition [$(Cu_{1.09–1.14}Fe_{0.02–0.05}Ni_{0.01–0.02})_{\Sigma 1.15–1.17}(Sn_{0.91–0.93}Sb_{0.07–0.09})_{\Sigma 1.00}$] and ranges of composition [Cu 0.97–1.19, Fe 0–0.13, Ni 0–0.04, Co <0.01, ΣMe 1.10–1.21, Sn 0.90–0.99, and Sb ≤0.01–0.10 *apfu*] have been documented in this study of sorosite from the Baimka deposit.

(2) The three sets of WDS analyses, obtained in this study using three different instruments and various sets of standards, are in excellent agreement with each other. These new compositional data lead to the following revision of the formula for the type-locality sorosite: $(Cu,Fe)_{1+x}(Sn,Sb)$, with $0.1 \leq x \leq 0.2$. The

excess Cu atoms likely occupy the trigonal-bipyramidal holes associated with interstitial sites of the NiAs-type lattice.

(3) The solid-solution series observed in this study extends from $Cu_{1+x}Sn$ (end-member sorosite) toward $Fe_{1+x}Sb$ (unnamed) and $Ni_{1+x}Sb$ (breithauptite), which both are isotypic with sorosite.

(4) The incorporation of Sb in sorosite is controlled by two mechanisms of substitution: [Cu + Sn = (Fe + Ni) + Sb] and Sb-for-Sn, which operates in sorosite poor in Fe and Ni.

(5) Relatively large grains of the type-locality sorosite are cryptically zoned in Fe, Ni, and Sb, the contents of which decrease from the center toward the margin. Values of the atom ratio 100 Fe / (Fe + Ni) also display characteristic, although more complex, variations in these zoned grains.

(6) Levels of Sb, Fe, and Ni generally decrease with decreasing temperature, and higher temperatures of crystallization promote the incorporation of these components in sorosite.

(7) Three main stages of crystallization of the type-locality sorosite are inferred. At stage 1, the large euhedral and zoned grains crystallized [from a Fe–Ni–(Sb)-rich core to a Fe–Ni–(Sb)-poor margin] from a late-stage or residual Sn–Sb–Cu–Fe–Ni-bearing liquid under conditions of low $f(O_2)$ and $f(S_2)$ during a normal drop in temperature. At stage 2, the large irregular or skeletal grains of sorosite (Fe–Ni-poor) crystallized nearly simultaneously with the Fe–Ni-poor periphery zones of the zoned crystals. At stage 3, the late generation of micrograins of sorosite (Ni–Fe-poor and poorer in Sb than the large grains) appeared in the host native tin, possibly at the eutectic point.

(8) A mineralized gabbro, gabbro–diorite, or clinopyroxenite associated with the Yegdegkychsky gabbro – diorite – monzonite – syenite complex, western Chukotka, is a likely source-rock for the sorosite-bearing placer mineralization.

(9) In the binary system Cu–Sn, sorosite crystallizes from a melt over the interval 415°–227°C. In nature, the upper boundary of this interval is slightly higher.

Acknowledgements

This study was made possible with financial support from the Natural Sciences and Engineering Research Council of Canada, which is gratefully acknowledged. We thank the journal referees, Drs. Chris J. Stanley and Frank Melcher, and Acting Editor Federica Zaccarini for their helpful and constructive comments. Stanislav Gornostayev provided samples of heavy-mineral concentrate in which the sorosite-bearing placer grains were found. We are grateful to Olli Taikina-aho (University of Oulu), Bo Johanson and Lassi Pakkanen (Geological Survey of Finland, Espoo) for their technical assistance with the EMP analyses. AYB thanks Prof. Kauko V.O. Laajoki for his support and efforts in the characterization of various ore minerals from the Baimkaplacer deposits, Chukotka, Russia.

References

Ageev, N.V. & Makarov, E.S. (1943): Physicochemical study of the phases with a nickel arsenide structure in the systems Fe–Sb–Ni and Fe–Sb–Co. *Bull. Acad. Sci. U.R.S.S., Classe Sci. Chim.*, 161-170.

Akimtsev, V.A. (1992): Native element minerals in magmatic rocks of the central part of the Mid-Atlantic Ridge. *Dokl. Akad. Nauk* **326**(6), 1026-1029 (in Russ.).

Aksenova, V.D., Dovgal, Yu.M. & Sterligova, V.Ye. (1970): Nickel–chromium mineralization of the Aluchin ultrabasic massif. *Geol. Geofis.* **2**, 23-33 (in Russ.).

Barkov, A.Y., Laajoki, K.V.O, Gornostayev, S.S., Pakhomovskii, Y.A & Men'shikov, Y.P. (1998): Sorosite, Cu(Sn,Sb), a new mineral from the Baimka placer deposit, western Chukotka, Russian Far East. *Am. Mineral.* **83**, 901-906.

Barkov, A.Y., Martin, R.F., Poirier, G., Tarkian, M., Pakhomovskii, Y.A. & Menshikov, Y.P. (2000a): Tatyanaite, a new platinum-group mineral, the Pt analogue of taimyrite, from the Noril'sk complex (northern Siberia, Russia). *Eur. J. Mineral.* **12**, 391-396.

Barkov, A.Y., Martin, R.F., Poirier, G. & Yakovlev, Y.N. (2000b): The taimyrite–tatyanaite series and zoning in intermetallic compounds of Pt, Pd, Cu, and Sn from Noril'sk, Siberia, Russia. *Can. Mineral.* **38**, 599-609.

Berlimble, D.G. & Gorodinskii, M.Ye. (1978): An ore-bearing gabbro–syenite complex in the western Chukotka. *In* Data on the Geology and Mineral Deposits of the Northeastern USSR **24**. Magadan, USSR (61-67; in Russ.).

Bhargava, M. K. & Schubert, K. (1973): Kristallstruktur von NiSn. *J. Less-Common Metals* **33**, 181-189.

Bowles, J.F.W. (1984): The distinctive low-silver gold of Indonesia and East Malaysia. *In* Gold '82: Geology, Geochemistry and Genesis of Gold Deposits (R.P. Foster, ed.). *Geol. Soc. Zimbabwe, Spec. Publ.* **1**, 249-260.

Chen, Lichang, Tang, Cuiqing, Zhang, Jianhong & Liu, Zhenyun (1994): Yuanjiangite: a new auriferous and stanniferous mineral. *Yanshi Kuangwuxue Zazhi* **13**, 232-238 (in Chinese).

Clark, A.H. (1972) A copper–tin alloy (η'–Cu_6Sn_5) from Panasqueira, Portugal. *Neues Jahrb. Mineral., Monatsh.*, 108-111.

Damman, A.H. & Kieft, C. (1990): W–Mo polymetallic mineralization and associated calc-silicate assemblages in the Gåsborn area, west Bergslagen, central Sweden. *Can. Mineral.* **28**, 17-36.

DEKOV, V.M., DAMYANOV, Z.K., KAMENOV, G.D., BONEV, I.K., RAJTA, I. & GRIME, G.W. (2001): Sorosite (η-Cu_6Sn_5)-bearing native tin and lead assemblage from the Mir zone (Mid-Atlantic Ridge, 26ºN). *Oceanol. Acta* **24**, 205-220.

DOVGAL, Yu.M. (1964): Ophiolite formations in the Aluchin horst. *In* Data on the Geology and Mineral Deposits of the Northeastern USSR **17**. Magadan, USSR (149-158; in Russ.).

EREMEEV, N.V., KONONOVA, V.A., MAKHOTKIN, I.L., DMITRIEVA, M.T., ALESHIN, V.G. & VASHCHENKO, A.N. (1988): Native metals in lamproites of central Aldan. *Dokl. Akad. Nauk SSSR* **303**, 1464-1467 (in Russ.).

FILIMONOVA, L.G., GORSHKOV, A.I., KORINA, E.A. & TRUBKIN, N.V. (1981): Occurrence of native metals in volcanic rocks of the southern Sikhote-Alin. *Dokl. Acad. Sci. USSR* **256**, 133-135.

FRIKH-KHAR, D.I., ASHIKHMINA, N.A., LUBNIN, E.N. & MURAVITSKAYA, G.N. (1986): Accessory native metals in carbonatites of the Cape Verde Islands. *Dokl. Akad. Nauk SSSR* **290**, 1481-1485 (in Russ.).

GAL'PERINA, T.N., ZELENIN, L.P., FEDOROVA, T.A., SIDORENKO, F.A. & GEL'D, P.V. (1977): Magnetic properties of mutual solid solutions of iron, cobalt, and nickel monoantimonides. *Fiz. Met. Metalloved.* **43**, 661-663 (in Russ.).

GELLER, W. (1939): The system iron–cobalt–antimony. *Arch. Eisenhuttenw.* **13**, 263-266.

GLAVATSKIKH, S.F. (1990): Native metals and intermetallic compounds in exhalation products of the Greater Tolbachik fissure eruption (Kamchatka). *Dokl. Akad. Nauk SSSR* **313**, 433-437 (in Russ.).

GORNOSTAYEV, S.S., CROCKET, J.H., MOCHALOV, A.G. & LAAJOKI, K.V.O. (1999): The platinum-group minerals of the Baimka placer deposits, Aluchin horst, Russian Far East. *Can. Mineral.* **37**, 1117-1129.

GORODINSKII, M.YE., TOLOKOL'NIKOV, A.I. & BERLIMBLE, D.G. (1982): On a relationship between placer gold and intrusive rocks. *In* Data on the Geology and Mineral Deposits of the Northeastern USSR **26**. Magadan, USSR (170-176; in Russ.).

GULEVICH, V.V. (1974): Subvolcanic rocks and ore deposits in the river Baimka basin. *In* Data on the Geology and Mineral Deposits of the Northeastern USSR **21**. Magadan, USSR (108-116; in Russ.).

GUROV, E.P. & KUDINOVA, L.A. (1987): Native metals from the Elgygytgyn meteorite crater (USSR). *Nov. Dannye Mineral.* **34**, 133-136 (in Russ.).

KAMINSKII, V.G. (1987): A porphyry copper deposit in the central part of the Baimka metallogenic zone. *Sovetsk. Geol.* **6**, 49-54 (in Russ.).

KAMINSKII, V.G. (1989): An integral geological-prospecting model for a porphyry copper deposit in the Baimka zone. *Sovetsk. Geol.* **11**, 46-56 (in Russ.).

KIM, A.A. & LESKOVA, N.V. (1988): Association of native lead and antimony with platinum-group metals in heavy concentrate complexes (central Aldan). *Dokl. Akad. Nauk SSSR* **303**, 458-463 (in Russ.).

KJEKSHUS, A. & WALSETH, K. P. (1969): Properties of the $Cr_{1+x}Sb$, $Fe_{1+x}Sb$, $Co_{1+x}Sb$, $Ni_{1+x}Sb$, $Pd_{1+x}Sb$, and $Pt_{1+x}Sb$ phases. *Acta Chem. Scand.* **23**(8), 2621-2630.

KOVALEV, S.G., SNACHEV, V.I., VYSOTSKII, I.V. & RYKUS, M.V. (1997): New type of precious metal mineralization in the western slope of the southern Urals. *Rudy Metall.* **6**, 27-32 (in Russ.).

KOVAL'SKIY, V.V. & OLEYNIKOV, O.B. (1985): Native metals and natural polymineralic alloys of copper, zinc, lead, tin, and antimony in the rocks of the Leningrad kimberlite pipe. *Dokl. Acad. Sci. USSR* **285**, 125-129.

KRIVITSKAYA N.N., SAKHAROVA M.S., RYABOV A.N. & TSEPIN, A.I. (1995): New data on the intermetallic compounds of tin. *Moscow Univ. Geol. Bull.* **50**(6), 65-70.

LARSSON, A.-K., STENBERG, L. & LIDIN, S. (1994): The superstructure of domain-twinned η'-Cu_6Sn_5. *Acta Crystallogr.* **B 50**, 636-643.

LARSSON, A.-K., STENBERG, L. & LIDIN, S. (1995): Crystal structure modulations in η-Cu_5Sn_4. *Z. Kristallogr.* **210**, 832-837.

LAVEROV, N.P., DISTLER, V.V., MITROFANOV, G.L., NEMEROV, V.K., KOVALENKER, V.A., MOKHOV, A.V., SEMEIKINA, L.K. & YUDOVSKAYA, M.A. (1997): Platinum and other native metals in ores of the Sukhoi Log gold deposit. *Dokl. Akad. Nauk* **355**, 664-668 (in Russ.).

LEFEVRE, G., ULRICH, M., BEHAR, F., SERVANT, C. & CIZERON, G. (1978): Structures des phases $Fe_{1+x}Sb$ et $FeSb_2$. *J. Less-Common Metals* **60**, 283-299.

LEUBOLT, R., IPSER, H., TERZIEFF, P. & KOMAREK, K.L. (1986): Nonstoichiometry in B_8-type NiSb. *Z. Anorg. Allg. Chem.* **533**, 205-214.

LIU, C. & WANG, Z. (1986): A mixture of ultramicro-native lead and tin. *Yanshi Kuangwuxue Zashi* **5**, 75-78 (in Chinese).

LYCHAGIN, P.P. (1985): The Aluchin massif and a problem with ophiolitic ultrabasics and gabbroids in Mesozoides of the northeastern USSR. *Tikhookean. Geol.* **5**, 33-41 (in Russ.).

NIKOLAEVA, E.P., GRIGORENKO, V.A., GAGARKINA, S.D. & TSYPKINA, P.YE. (1970): New natural intermetallic compounds of tin, antimony, and copper. *Zap. Vses. Mineral. Obshchest.* **99**, 68-70 (in Russ.).

NOVGORODOVA, M.I. (1983): Association of native metals in hydrothermal deposits. *In* Problems of Petrology, Mineralogy and Ore Genesis (F.V. Chukhrov & V.I. Rekharskii, eds.). Nauka, Moscow, USSR (154-159; in Russ.).

OKRUGIN, A.V., OLEINIKOV, B.V., ZAYAKINA, N.V. & LESKOVA, N.V. (1981): Native metals in trap rocks of the Siberian platform. *Zap. Vses. Mineral. Obshchest.* **110**, 186-204 (in Russ.).

PEKOV, I.V. (1993): Minerals of nickeline–breithauptite series in the Belorechensk deposit (northern Caucasus). *Zap. Vser. Mineral. Obshchest.* **122**(3), 44-49 (in Russ.).

RAZIN, L.V. & SIDORENKO, G.A. (1989): Anyuiite, $AuPb_2$, a new intermetallic compound of gold and lead. *Mineral. Zh.* **11**(4), 88-96 (in Russ.).

RICHTER, F.W. & SCHMIDT, K. (1975): Mössbauer-spectroscopic studies in the $Fe_{1+x}Sb$ system with NiAs-structure. *Z. Naturforsch.* **30A**, 1621-1626.

ROSE, D. (1981): New data for stistaite and antimony-bearing η-Cu_6Sn_5 from Rio Tamaná, Colombia. *Neues Jahrb. Mineral., Monatsh.*, 117-126.

RUDASHEVSKII, N.S., DMITRENKO, G.G., MOCHALOV, A.G. & MEN'SHIKOV, YU.P. (1987): Native metals and carbides in alpine-type ultramafic rocks of the Koryak Upland. *Mineral. Zh.* **9**(4), 71-82.

RUDASHEVSKII, N.S., KRETSER, YU.L., ANIKEEVA, L.I., ANDREEV, S.I., TOROKHOV, M.P. & KAZAKOVA, V.E. (2001): Platinum minerals in ferromanganese oceanic crusts. *Dokl. Akad. Nauk* **378**, 246-249 (in Russ.).

SAUNDERS, N. & MIODOWNIK, A.P. (1990): The Cu–Sn (copper–tin) system. *Bull. Alloy Phase Diagrams* **11**, 278-287.

SEREDIN, V.V., GENERALOV, M.E. & EVSTIGNEEVA, T.L. (1998): New discovery of native tantalum. *Dokl. Akad. Nauk* **360**, 791-795 (in Russ.).

SHTERENBERG, L.E. (1997): Native metals in a pumice (southeast Kamchatka). *Dokl. Akad. Nauk* **355**, 520-523 (in Russ.).

SURNIN, A.A. & OKRUGIN, A.V. (1989): Basic–ultrabasic magmatism of the South Anyuy structural unit. *Tikhookean. Geol.* **5**, 10-18 (in Russ.).

TASAKI, M. (1929): Ternary system: copper–tin–antimony. *J. Inst. Metals* **42**, 447.

VOLCHKOV, A.G., SOKIRKIN, G.I. & SHISHAKOV, V.B. (1982): Geological structure and ore composition of the Anyuy porphyry copper deposit (northeastern USSR). *Geol. Rudnykh Mestorozhd.* **24**, 89-94 (in Russ.).

WESTGREN, A. & PHRAGMÉN, G. (1928): Röntgenanalyse der Kupfer–Zinn-legierungen. *Z. Anorg. Allg. Chem.* **175**, 80-89.

WEVER, H. & WINTERMANN, G. (1961): Bonding conditions in intermetallic phases of the NiAs-type. *Z. Metallk.* **52**, 329-336.

YAMAGUCHI, K., YAMAMOTO, H., YAMAGUCHI, Y. & WATANABE, H. (1972): Antiferromagnetism of Fe_{1+x} Sb. *J. Phys. Soc. Japan* **33**, 1292-1295.

YASHIRO, T., YAMAGUCHI, Y., TOMIYOSHI, S., KAZAMA, N. & WATANABE, H. (1973): Magnetic structure of Fe_{1+x} Sb. *J. Phys. Soc. Japan* **34**, 58-62.

YUSHKIN, N.P., GORDIENKO, V.V., KOVALEVA, O.V. & LIKBERG, P.L. (2000): Solid hydrocarbons with native metals from Glasberget pegmatite, Sweden. *Zap. Vser. Mineral. Obshchest.* **129**, 1-12 (in Russ.).

Received February 4, 2006, revised manuscript accepted March 8, 2006.